

## Photoenhancement of Luminescence in Colloidal CdSe Quantum Dot Solutions

Marcus Jones, Jovan Nedeljkovic, Randy J. Ellingson, Arthur J. Nozik, and Garry Rumbles\*

National Renewable Energy Laboratory, 1617 Cole Boulevard, Golden, Colorado 80401-3393

Received: June 6, 2003; In Final Form: July 29, 2003

Enhancement of the photoluminescence (PL) of colloidal CdSe and (core)shell (CdSe)ZnS quantum dots has been observed when the dots are illuminated above the band-gap energy. The effect occurs in dots suspended in a variety of organic or aqueous environments. During periods of constant illumination, the exciton PL quantum yield was found to reach a value of up to 60 times that of the solution of as-prepared quantum dots and, if illumination continued, subsequently declined slowly because of photooxidation. When returned to the dark, the PL reverted to near its original value. The rate and magnitude of photoenhancement are found to depend on the illumination wavelength, the presence of a ZnS shell, the solvent environment, and the concentration of surfactant molecules. Time-resolved measurements of the fluorescence decay reveal multiexponential kinetics and an average lifetime that lengthens during the illumination period and shortens when quantum dots are returned to darkness. It is postulated that the stabilization of surface trap states, lengthening their average lifetime, could occur by a light-activated rearrangement of surfactant molecules, thus increasing the probability of thermalization back to the lowest emitting exciton state and enhancing the quantum dot PL.

### Introduction

Optical spectroscopy of colloidal semiconductor quantum dots has enabled a good understanding of the electronic properties of these unique systems. In particular, there is interest in the effects of quantum dot composition and surface environment on the confinement of exciton states and subsequently on the luminescence quantum yield. The energy of quantum dot exciton photoluminescence (PL) is easily controlled by varying the dot sizes; however, the factors that control the efficiency at which quantum dot excitons undergo radiative versus nonradiative decay have not yet been manipulated.

It has been found that exciton PL intensity in CdSe quantum dots may be altered by a variety of techniques. Capping the CdSe core with a shell of higher-band-gap material such as ZnS<sup>1–3</sup> was found to increase the luminescence quantum yield significantly by passivating the CdSe surface traps. Similarly, surfactant molecules bound to the CdSe dots affect the efficiency of radiative versus nonradiative exciton decay; for example, a hole acceptor, *n*-butylamine, will diminish the exciton PL intensity<sup>4</sup> by removing core holes and rapidly trapping them at the surface of the dots. More recently, a detailed investigation of the factors governing the PL efficiency of CdSe nanocrystals during synthesis<sup>5</sup> enabled the reproducible production of high quantum yield (50–85%) dots by selecting reaction conditions that minimized surface disorder and surface degradation and enabled good passivation of the dots. Photochemical etching<sup>6</sup> with HF has been used to enhance the quantum yield of InP (but not CdSe) dots by removing surface hole traps by attack with fluorine ions in solution.

Observations of bleaching and the blue shift of the exciton PL have been reported<sup>7</sup> in CdSe and (CdSe)ZnS (core)shell quantum dots exposed to intense illumination. Photobleaching was found to occur about 4 times faster in air (together with an ~30-nm PL blue shift) than in N<sub>2</sub>. In addition, the PL in air was reported to be initially more intense than that in N<sub>2</sub>, which

was possibly caused by O<sub>2</sub> quenching of deep trap emission. Partially reversible photodarkening has also been observed in CdSe cluster molecules with up to 32 Cd atoms.<sup>8</sup> This was attributed to their temporary charging, which would quench the emission via efficient nonradiative Auger recombination of the electron–hole pair induced by the excess charge.

Emission intermittency or “blinking” has been recorded in CdSe and (CdSe)ZnS quantum dots,<sup>9–11</sup> and both Auger autoionization of two e<sup>–</sup>h<sup>+</sup> pairs and thermal ionization of a single e<sup>–</sup>h<sup>+</sup> pair have been found to contribute to the rate of blinking.<sup>10</sup> This periodic darkening and brightening is a single-dot property and is not exhibited in the ensemble luminescence. In what may be a related effect, the use of correlated atomic-force and single-particle fluorescence microscopy<sup>12</sup> revealed that a significant proportion of (CdSe)ZnS quantum dots in an ensemble are “dark” (i.e., they do not undergo radiative decay and therefore reduce the quantum yield of the ensemble).

Photoenhancement of CdSe quantum dot PL has been reported previously in aqueous solution,<sup>13</sup> close-packed nanocrystalline films,<sup>14,15</sup> and monolayers.<sup>16</sup> The latter study found that the intensity of exciton PL in monolayers of hexadecylamine (HDA)-capped CdSe quantum dots (also trioctylphosphine (TOP)/trioctylphosphine oxide (TOPO)-capped and (CdSe)ZnS core–shell dots) was found to increase under broad-band (400–490 nm) illumination. In addition, the exciton PL peak underwent a blue shift and a narrowing with subsequent rebroadening. The PL of the smallest CdSe dots was found to rise the most quickly, and those that were capped with a ZnS shell were more resistant to enhancement. These effects were observed only under “wet” O<sub>2</sub> or N<sub>2</sub> and were not seen in vacuum or in the presence of dry gases. It was therefore suggested that the PL enhancement was due to the photopassivation of charge-carrier traps by the adsorption of H<sub>2</sub>O molecules to the surface of the dots.

Photoinduced recovery of PL has also been observed in organically capped CdSe quantum dots after they have been darkened by heating to 200 °C.<sup>17</sup> This dark state, attributed to

\* Corresponding author. E-mail: grumbles@nrel.gov.

a surface transformation, was stable for months or until the luminescence was recovered by above-band-gap illumination. The dynamics of PL recovery were found to follow stretched exponential dynamics. In this paper, we describe a similar, but quasi-reversible, photoenhancement effect in colloidal CdSe and (CdSe)ZnS core-shell quantum dots attached to a variety of surfactant molecules in aqueous and nonaqueous environments.

We found that the relaxation mechanisms of the exciton could play an integral role in the photoenhancement effect. These have previously been monitored by femtosecond fluorescence up-conversion<sup>18</sup> and transient absorption<sup>19</sup> measurements, and it is clear that charge-carrier recombination at surface trap states is an important component of the relaxation process. Optically detected magnetic resonance studies of the surface/interface properties in CdSe(CdS) (core)shell dots and CdSe dots capped with TOPO or formed within a phosphate glass<sup>20</sup> have provided useful information about the composition of these trap states and have revealed that photogenerated electrons and holes may be trapped at the core/shell interface (CdSe/CdS) or at external adatoms on the surface of the dots.

## Experimental Section

Colloidal, nanocrystalline CdSe was synthesized using a previously published procedure<sup>21</sup> that utilizes CdO as a cadmium precursor. A ZnS shell was subsequently added by the dropwise addition of Zn(CH<sub>3</sub>)<sub>2</sub> and S[Si(CH<sub>3</sub>)<sub>3</sub>]<sub>2</sub> to the colloidal CdSe solution at 170 °C. After 30 min, the solution was allowed to cool slowly. The (CdSe)ZnS dots used in these experiments were estimated to have a core diameter of ~33 Å. This value was obtained from their absorption spectrum using results in Murray et al.<sup>22</sup> and adjusted, with reference to Dabbousi et al.,<sup>3</sup> by assuming a 5-Å (1 to 2 monolayer) ZnS shell.

Solutions of (CdSe)ZnS nanocrystals were purified by precipitation with a minimum amount of methanol followed by centrifugation and removal of a pale-yellow supernatant. The (CdSe)ZnS was redissolved in a 0.01 M solution of TOPO in toluene, and the process was repeated. After two or three washes, the quantum dots were finally dissolved in either a toluene/TOPO or a hexane/TOPO solution. The degassing process was repeated three or four times and involved freezing the solution in liquid nitrogen, pumping to a pressure of <10<sup>-4</sup> Torr, and then allowing the solution to melt slowly.

Photoluminescence (PL) spectra were recorded using a Fluorolog-3 (JYHoriba) spectrometer that utilized a CCD detection system and enabled the accumulation of entire spectra in a few seconds or less. Monochromatic excitation light was generated by either a Xe arc lamp with a double monochromator or an air-cooled CW Ar<sup>+</sup> laser (Ion Laser Technology ILT500) with an output of 13–16 mW of 488-nm light. The laser light was dispersed onto the sample with a beam diameter of ~5 mm. Fluorescence light was collected at 90° relative to the excitation beam, passed through a single monochromator containing a 150 line/mm grating, and imaged on the liquid-nitrogen-cooled CCD array. All PL spectra were corrected for the spectral output of the excitation source and for the spectral response of the detection optics. Quantum yields were calculated relative to Lumogen F Orange 240, a perylene dye assumed to have a value close to unity.

Steady-state absorption spectra were recorded on a Cary 500 double-beam spectrophotometer at 1 nm spectral resolution.

Fluorescence decay signals were measured using the technique of time-correlated single-photon counting (TCSPC). The spectrometer comprised a pulsed, picosecond diode laser (IBH NanoLED-10) operating at a wavelength of 438 nm and a

repetition rate of 1 MHz. Emission was detected at 90° relative to excitation by focusing the emission onto the slits of a 0.25-m monochromator (SPEX minimate) and was subsequently detected by a photon-counting photomultiplier tube (Hamamatsu H6279). The PMT output was amplified using a 1-GHz amplifier (Philips model 6954) and then shaped using a constant-fraction discriminator (Ortec, Tennelec model 583) and fed into the starting input of a time-to-amplitude converter (TAC, Ortec, model TC864), which was operated in reverse mode.<sup>23</sup> The stop input to the TAC was supplied by an output directly from the pulsed laser diode controller (IBH NanoLED-C). The TAC output was fed to a multichannel analyzer (Oxford Instruments PCA3-8K) operating in pulse-height analysis mode. The instrument response function (IRF) from this system when scattering the excitation light from a dilute solution of colloidal silica was determined to be 220 ps. Using a nonlinear, least-squares iterative deconvolution procedure employing the Marquardt minimization routine, the influence of the IRF could be removed from the measured luminescence decay curves to reproduce the true decay kinetics with a temporal resolution of ~30 ps.

Transient absorption spectra were measured using a system that was previously described in detail.<sup>24</sup> It is based on a Clark-MXR CPA-2001 regeneratively amplified Ti:sapphire laser operating at 989 Hz. The 775-nm output pulses pump a TOPAS optical parametric amplifier capable of output in the range of 290 nm to 2.4 μm; in addition, a fraction of the 775-nm pulse train is focused onto a 2-mm sapphire window to generate white-light probe pulses, which range from ~490 to 950 nm. The visible pump and white-light probe pulses were focused to spot sizes of ~500 and 125 μm, respectively. Spatially filtering the pump beam was used to improve the transverse-mode quality. Standard transient absorption measurement techniques were utilized in which a visible pump pulse photoexcites the dots at or above the first exciton transition and the white-light pulse probes the induced change in absorption at a specific energy as selected by a 0.25-m monochromator (CVI DK240).

## Results

When a solution of (CdSe)ZnS core-shell quantum dots capped with TOPO in a 0.01 M TOPO/toluene solution was subjected to four periods of continuous illumination at 488 nm, the intensity of PL was found to undergo significant enhancement. The sample was exposed to two periods of illumination on day one and two more periods the next day. Each period lasted approximately 2.5 h. Spectral traces, acquired at regular intervals during the first illumination period and corrected for lamp intensity and detector sensitivity, are plotted in Figure 1a. The separation of exciton, deep trap, and Raman contributions to the total PL intensity was achieved by carefully fitting the individual spectra to multiple Gaussian functions and enabled values for the exciton PL intensity, peak energies, and full widths at half-maximum (fwhm) to be extracted. The evolution of the exciton quantum yield during four separate periods of illumination of the same sample is illustrated in Figure 1b, and the peak energies and fwhm are plotted in Figure 2.

A stretched exponential function of the form in eq 1 may be used to model the rise in the PL quantum yield:

$$y = y_0 + A \exp\left[-\left(\frac{t}{\tau}\right)^\beta\right] \quad (1)$$

where  $t$  is the time of illumination and is proportional to the number of photons absorbed. Values of  $y_0$ ,  $A$ ,  $\beta$ , and  $\tau$  are tabulated in Table 1a for each of the four illumination periods in Figure 1b.

**TABLE 1: Best-Fit Values of  $y_0$ ,  $A$ ,  $\beta$ , and  $\tau^a$** 

	(a) illumination period (Figure 1b)				(b) (CdSe)ZnS/TOPO (Figure 4) in solution with		
	1	2	3	4	tol	tol/MeOH	hex/MeOH
$y_0$	7.26	19.24	14.44	16.58	5.9861	13.585	27.06
$A$	-6.89	-14.80	-11.36	-7.06	-5.7904	-13.206	-24.52
$\tau$	6820	51179	8051	10937	9754	7462	5077
$\beta$	1.23	0.51	0.69	0.50	0.93	0.73	0.92

<sup>a</sup> These were obtained by fitting the stretched exponential function in eq 1 to the quantum yield photoenhancement curves plotted in Figures 1b and 4.

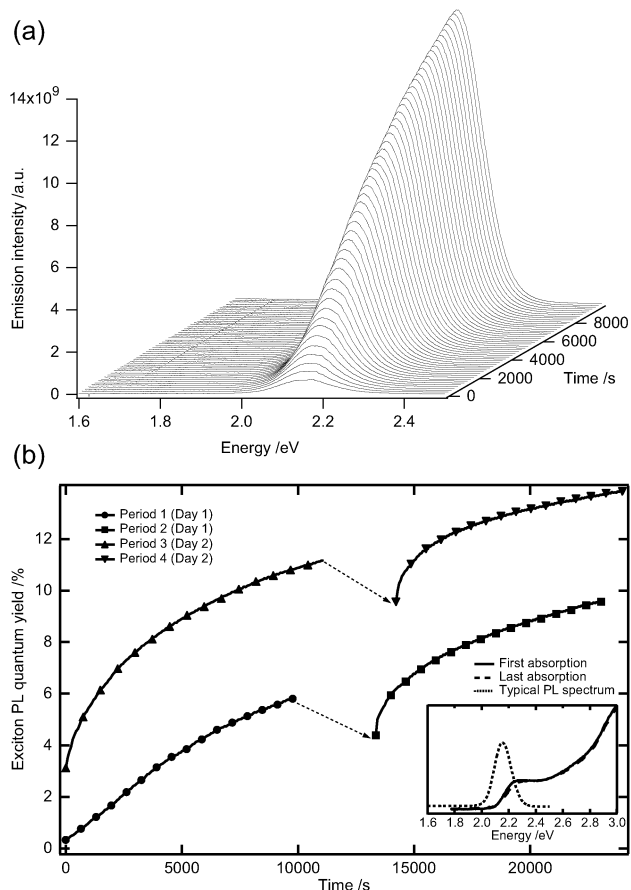


**Figure 1.** (a) Representative series of luminescence spectra and (b) the relative fitted exciton emission intensities for a sample of (CdSe)-ZnS quantum dots in 0.01 M TOPO/toluene illuminated with 488-nm light. The inset to b depicts a typical fluorescence spectrum with two absorption spectra taken before the first and after the fourth illumination period.

Time-correlated single-photon counting experiments were performed at the beginning and end of every period in Figure 1b. The quantum dot solutions were excited at 438 nm, and the PL decay was monitored at the peak of the exciton emission ( $\sim 578$  nm). The decays are plotted in Figure 3, and the data was analyzed using the multiexponential model described by eq 2:

$$I(t) = \sum_{i=1}^n \alpha_i \exp\left(-\frac{t}{\tau_i}\right) \quad (2)$$

where  $\tau_i$  represents the decay times,  $\alpha_i$  represents the amplitudes of the components at  $t = 0$ , and  $n$  is the number of decay times. Decay waves generated using eq 2 were found to produce a good fit to the data in Figure 3 when five exponential components were used (i.e.,  $n = 5$ ). The resulting decay times,  $\tau_i$ ; their fractional contributions,  $Y_i$ ; the average decay lifetimes,

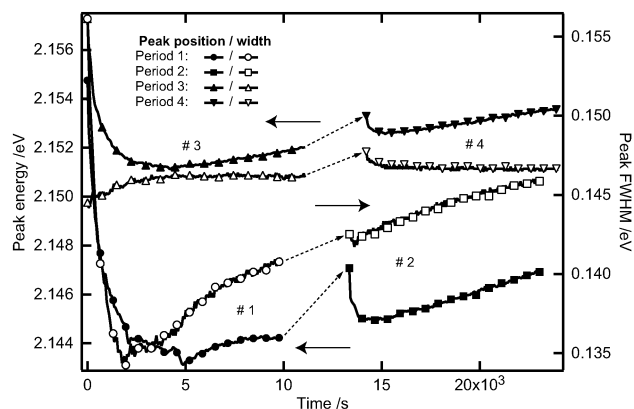


**Figure 2.** Energy shift of the exciton PL peak maxima and fwhm during each of the four illumination periods in Figure 1b.

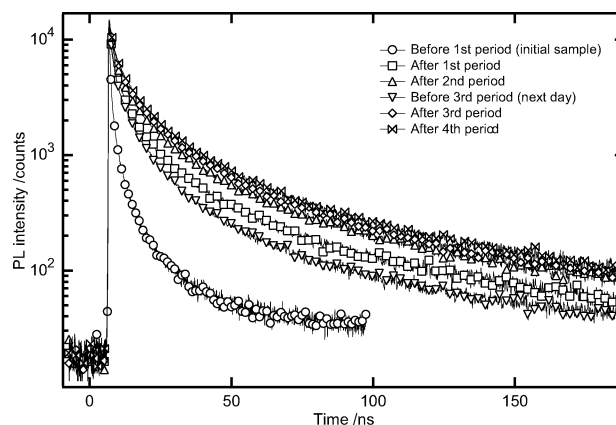


**Figure 3.** Fluorescence decay kinetics of (CdSe)ZnS (core)shell colloidal quantum dots, taken before and after each of the illumination periods in Figure 1.

$\bar{\tau}$  (calculated from eq 3); and the values of the goodness-of-fit parameter,  $\chi_R^2$ , are listed in Table 2 for each of the decays. The reduced chi-square values,  $\chi_R^2$ , are all close to 1.0, indicating a good fit to each data set. Note that five exponential components all produced fits with  $\chi_R^2 \leq 1.10$ ; four components typically resulted in  $\chi_R^2 \approx 1.5$ .

$$\bar{\tau} = \frac{\sum_{i=1}^n \alpha_i \tau_i^2}{\sum_{i=1}^n \alpha_i \tau_i} \quad (3)$$

Interesting effects were observed when methanol was added to a toluene or hexane solution of (CdSe)ZnS quantum dots, and a comparison of the results of these experiment with measurements taken using an identical quantum dot concentration in toluene/TOPO (no methanol) solution is presented in Figure 4. The quantum yield rises have been fit to the stretched

TABLE 2: Fitted Decay Lifetime Components

<i>i</i>	day 1						day 2					
	initial sample		after period 1		after period 2		before period 3		after period 3		after period 4	
	$Y_i/\%$	$\tau_i/\text{ps}$	$Y_i/\%$	$\tau_i/\text{ps}$	$Y_i/\%$	$\tau_i/\text{ps}$	$Y_i/\%$	$\tau_i/\text{ps}$	$Y_i/\%$	$\tau_i/\text{ps}$	$Y_i/\%$	$\tau_i/\text{ps}$
1	15.0	72.3	2.9	54.2	2.5	84.2	3.7	56.5	1.8	93.2	1.7	100.3
2	18.0	473.8	9.6	722.7	8.7	982.4	13.2	793.7	7.7	1097	7.3	1110
3	26.3	2111	28.0	3725	27.1	4796	31.3	3966	26.1	5370	24.7	5231
4	24.8	7991	37.2	14570	36.6	16 950	34.0	14 090	37.8	18 960	38.5	17 710
5	15.9	51 940	22.3	68 930	25.1	74 600	17.7	66 870	26.7	91 390	27.8	78 550
$\bar{\tau}/\text{ps}$	10 870		21 920		26 300		17 980		33 010		30 030	
$\chi_R^2$	1.02		1.10		1.06		1.02		1.10		1.06	

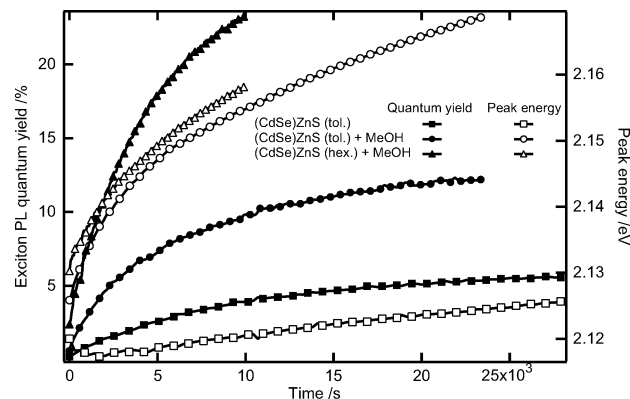


**Figure 4.** Effect of methanol on the rate and magnitude of the photoenhancement of the (CdSe)ZnS PL quantum yield and exciton-peak emission energy.

exponential in eq 1, and the results are presented alongside those produced in the absence of methanol in Table 1, section b. In addition, enhancement effects were observed for a wide range of CdSe quantum dot preparations, including four sizes of CdSe dots (no ZnS shell) in a toluene/TOPO or hexane/TOPO solution, both aerated and degassed, and (CdSe)ZnS dots capped with mercaptopropionic acid or mercaptoethanol in water.

Transient absorption kinetics of (CdSe)ZnS quantum dots in hexane were measured before, during, and after a 115-min period of illumination with 532-nm light at a power of 27 mW for 103 min followed by 108 mW for the last 12 min. A 488-nm pump pulse was used to excite the dots, and the bleach decay kinetics were probed at 571 nm. Measurements taken before illumination, after the addition of 100  $\mu\text{L}$  of (immiscible) methanol, and after 115 min of illumination are plotted in Figure 5a. In addition, transient absorption spectra, measured 25 ps after the 488-nm pump beam and taken before and after the illumination period, are plotted with the corresponding PL spectra (recorded on a different system and therefore uncorrected) in Figure 5b.

## Discussion

Typical results from the initial illumination experiments shown in Figure 1 and Figure 2 reveal a partially reversible photoactivated PL enhancement effect. After an initial  $\sim 1700\%$  PL increase during the first illumination period, the sample was kept in darkness for  $\sim 1$  h, and the PL was observed to decay by 26%. Subsequent illumination (periods 2–4 in Figure 1b) resulted in the further enhancement of the exciton PL quantum yield followed by its repeated diminution in darkness. Overnight, between periods 2 and 3, the PL returned to 9.5 times its original value, indicating either that the relaxation process is very slow or that some irreversible change to the dots' composition had occurred. (We typically found that after photoenhancement experiments the PL intensity approached and could eventually

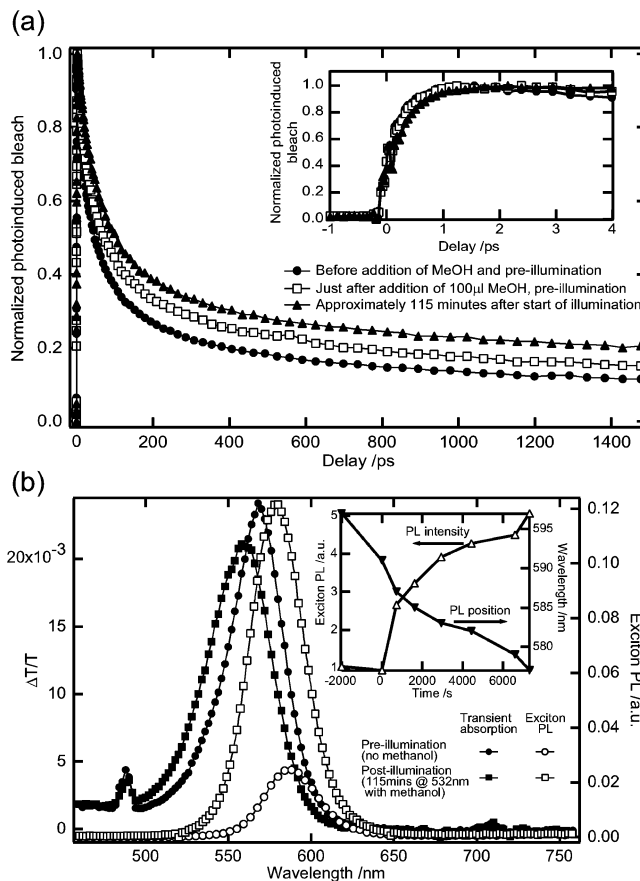


**Figure 5.** (a) Bleach decay kinetics probed at 571 nm (2.17 eV) and (b) transient absorption spectra measured 25 ps after the pump beam for (CdSe)ZnS (core)shell quantum dots in a 0.01 M TOPO/hexane solution.

become less than that of the original sample.) Over the four periods, the exciton PL was observed to brighten by a factor of 42 and reach a quantum yield of 13.9%.

The stretched exponential form observed in the photoenhancement of the PL quantum yield is seen in the dynamics of a wide variety of systems with strongly coupled hierarchical degrees of freedom<sup>25</sup> and in disordered systems.<sup>26</sup> For example, the dynamics of PL photoenhancement could be described by the transformation of the quantum dot surface in hierarchical steps, in which slow steps depend on the completion of the previous faster step. The results presented in Table 1 reveal an increase in  $\tau$  and a decrease in  $\beta$  from periods 1 to 2 and 3 to 4 and indicate that the initial rise in PL intensity is faster when the sample has recently been illuminated, as if the previous illumination period sensitizes the dots to further phototransformations. This sensitization appears to decrease with the time spent in darkness because the values of  $\tau(\beta)$  decrease(increase) between periods 2 and 3.

All four periods of illumination resulted in an initial reddening of the PL followed by its subsequent steady shift to the blue, as shown in Figure 2. A change in dot size could lead to such a change, but it has also been reported<sup>27,28</sup> that the wavelengths of optical absorption and emission bands are affected by the presence of charge on the surface of the quantum dots, resulting in a Stark effect energy shift. It is therefore plausible that charge, localized in surface traps, could produce the initial PL red shift and that a slow contraction of the dot diameter could then account for the eventual blue shift. Absorption data shown in the inset to Figure 1b reveals a slight blue shift of the exciton absorption and confirms a slight reduction in average dot sizes. The exciton peak width, shown in Figure 2, first narrows by approximately 13% in the first 30 min of illumination and then gradually rebroadens to eventually level out at 94% of its initial value, indicating again that at least two distinct processes are occurring when the dots are placed under illumination.

The kinetics of PL decay, measured by TCSPC and plotted in Figure 3, lengthen when the sample is illuminated and shorten when it is kept in the dark. Average lifetimes increase from 10.9 to 33.0 ns after the third illumination period. The fourth period results in a drop in the average lifetime to 30.0 ns, as modeled by the five-exponential fit: this could indicate the start of a photooxidative bleaching process.<sup>7</sup> Both multiexponential and stretched exponential functions were utilized in an attempt to model the TCSPC data. As described, the multiexponential functions fit the data well, but interestingly, stretched exponentials were found not to fit the PL decays. Stretched exponential functions arise from a continuous distribution of exponential decays,<sup>29</sup> whose width and shape are determined by  $\beta$  in eq 1. This finding, therefore, appears to point to the existence of a number of discrete relaxation pathways, each with an individual associated lifetime. The exact number and identity of these pathways are unknown, and the five-exponential fit could be masking a decay mechanism with many more than five possible routes.

Several possible models could be used to explain the photoenhancement of CdSe quantum dot PL: (1) the dark dots<sup>12</sup> in the ensemble may be induced to start fluorescing; (2) the blinking<sup>9–11</sup> effect may be in some way inhibited to reduce the amount of “off” time; or (3) the illumination could cause a chemical change in the luminescent dots that results in higher fluorescence efficiency during their “on” periods. The increase in average PL decay lifetimes (Figure 3) could certainly occur in models 3 and 1 if the previously dark dots have a longer PL lifetime,  $\bar{\tau}$ , than the already present luminescent dots. Model 2 involves a population of dots that are transiently on or off; therefore, increasing the on periods should not cause a change in the decay lifetimes. A simple increase in the e–h pair recombination efficiency would not result in an increase (and could, in fact, lead to a decrease) in the observed fluorescence decay lifetimes, so this mechanism can be discounted. Additionally, the gradual evolution of peak energies (Figure 2) suggests that the luminescent dots themselves must be undergoing a photoinduced chemical change that causes the PL efficiency (and not the on period of blinking dots) to increase.

Electronic structure calculations within the framework of both the effective mass approximation<sup>30,31</sup> and many-body pseudopotential theory<sup>32</sup> predict the band edge of CdSe quantum dots to contain five states within  $\sim 20$  meV for 33-Å dots. These states are labeled by their total angular momentum projection,  $F_m = m_e + m_j$ , where  $m_{e(j)}$  is the electron(hole) angular momentum projection. These states are illustrated on the left side of Figure 6; “U” and “L” denote the upper and lower states

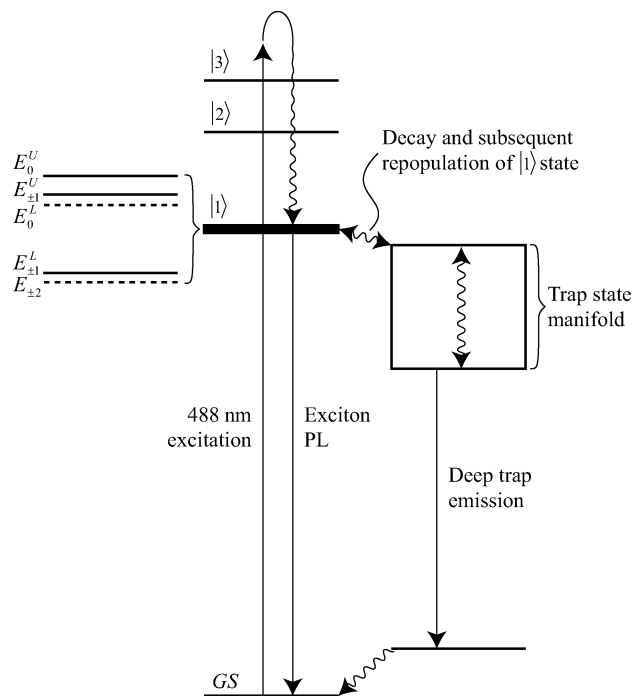


**Figure 6.** Schematic illustration of the postulated decay route of an exciton generated in (CdSe)ZnS quantum dots.

with the same angular momentum, and the dashed lines denote optically spin-forbidden states. The oscillator strength of the lowest-energy forbidden radiative transition (from the  $E_{\pm 2}$  state, lying just 2 meV below  $E_{\pm 1}^L$  in 33-Å CdSe quantum dots<sup>33</sup>) is predicted to be at least  $10^6$  times smaller than that of the next-highest allowed transition.

Once formed, excitons in (CdSe)ZnS quantum dots decay back to the lowest exciton state, labeled |1> in Figure 6, in less than 1 ps, as evidenced by the rise time of the bleach signals in the inset to Figure 5a. These rise times are not noticeably affected by the ongoing illumination. A portion of |1> is expected to decay rapidly to the quantum dot ground state, GS, in a time that is reflected by the fastest components,  $\tau_1$ , of the multiexponential fits to the PL decay in Table 2 (i.e.,  $\leq 100$  ps). Some of the quantum dots will undergo nominally spin-forbidden decay to the lowest component of |1>,  $E_{\pm 2}$ . This state will then either return radiatively or nonradiatively to GS or thermalize back to the next-highest spin-allowed states. The involvement of the dark exciton state is expected to lengthen the average measured luminescence lifetime,<sup>33</sup> but it is not clear how above-band-gap illumination could further extend this lifetime and enhance the PL.

An alternative relaxation route involves the formation of nonradiative surface states consisting of trapped electrons or holes that have already been mentioned with regard to peak energies. These states, depicted on the right of Figure 6 (a similar representation is used by Bawendi et al.<sup>34</sup>), may either thermalize back to emitting states in |1>, resulting in delayed exciton luminescence, or undergo further nonradiative decay to levels that eventually produce the very weak deep-trap emission around 1.6 eV. The photoinduced lengthening of the PL decay could then result from an increase in the lifetimes of these nonradiative trap states caused by a light-induced rearrangement (or addition) of surfactant molecules that serve to stabilize the  $e^-$  or  $h^+$  traps, both of which have been shown to occur in CdSe.<sup>19</sup> Lengthening the average trap-state lifetime will, in addition, increase the

chance that thermalization may occur back to an emitting  $|1\rangle$  state and therefore lead to the observed photoenhancement effect.

Previous studies<sup>20</sup> have tried to pinpoint the nature of the trapping sites on CdSe quantum dots in a variety of environments using optically detected magnetic resonance. Studies on CdSe(CdS) and CdSe quantum dots indicate that photogenerated electrons and holes in the CdSe(CdS) quantum dots may be trapped at the CdSe–CdS interface (i.e., between the core and shell). CdSe quantum dots embedded within a phosphate glass were found to possess dangling bonds and external adatoms at the surface, which may act as nonradiative traps for the photogenerated carriers. Similar interface trap sites could play an important role in the photoenhancement effect as they become better passivated by the rearrangement or detachment of either surfactant molecules or the ZnS shell.

Figure 4 shows the effect of methanol on the rate of photoenhancement and on the photoinduced shift in the exciton peak energy. Both toluene/methanol and hexane/methanol systems show an accelerated growth of the PL quantum yield compared to that of toluene-only quantum dot solutions. The immiscible hexane/methanol system shows the largest effect, reaching a quantum yield of 23% in 165 min, and both of the methanol systems show similar time-dependent peak-energy behavior, with the toluene/methanol solubilized dots undergoing a 43-meV blue shift. These data suggest that methanol or, in concurrence with the findings of previous enhancement studies,<sup>16</sup> the water present in the methanol solution could be acting as a surfactant, stabilizing the hole on the surface of the quantum dots by coordination through the oxygen. Dissolved methanol (or water) could also stabilize surface charge by increasing the local dielectric constant of the surrounding solution. Note that the quantity of methanol used and the concentration of quantum dots in solution were not enough to result in significant dot precipitation.

The bleach signal decay, plotted in Figure 5a, lengthens upon the addition of the immiscible layer of methanol and then again after 115 min of illumination at 532 nm. The latter effect mirrors the lengthening of the PL lifetime measured by time-correlated single-photon counting experiments, but the methanol-induced shift was unexpected. The addition of methanol also causes the PL peak (Figure 5b) to shift  $\sim 21$  meV (6 nm) to the blue. The Stokes shift of the emission line relative to the absorption in CdSe dots with positive and negative charges present on the surface has been calculated using a many-body approach based on single-particle pseudopotential wave functions.<sup>27</sup> When there are one or more positive charges, the Stokes shift is predicted to be relatively large ( $\sim 50$ – $70$  meV), but when the dot is neutral, the Stokes shift is small (a few meV). If methanol acts to passivate hole traps, it could effectively lower the surface charge and therefore lead to the observed blue shift in the exciton PL.

## Conclusions

The illumination of (CdSe)ZnS (core)shell colloidal quantum dots in hexane or toluene solution has been observed to increase their PL quantum yield from 0.3 to 13.8%. The addition of methanol to the dot solution resulted in the acceleration and amplification of the photoenhancement effect. The fluorescence decay kinetics were measured and found to be multiexponential, and the average fluorescence decay lifetimes were observed to lengthen under illumination. Transient bleach kinetics were found to mirror the fluorescence decay kinetics and lengthened upon irradiation as well as upon the addition of methanol. The

transient absorption spectra showed a shift to the blue that was similar to the shift observed for the PL in methanol/hexane solution.

An interpretation that fits the measured data involves the nonradiative decay of excitons to trap states that exist long enough to ensure that there is a significant possibility of their thermalization back to spin-allowed states in the exciton ground-state manifold,  $|1\rangle$ . Photoinduced rearrangement of TOPO groups on the dot surface or the addition of surfactant molecules such as methanol could stabilize these trap states and increase their lifetime. If this happens, then the probability of their transforming back to  $|1\rangle$  rises relative to the probability of further decay, thus lengthening the dots' luminescence lifetimes and causing an enhancement of exciton PL.

The precise nature of the passivation process is not yet understood, but regardless of the model used for interpretation, it is clear that the effect must be taken into account when considering experimental results that have involved lengthy periods of dot illumination. This effect may explain the anomalous difference between absorption and PLE spectra observed for both InP<sup>35</sup> and CdSe.<sup>36</sup>

**Acknowledgment.** This work was supported by the U.S. Department of Energy (DOE) Solar Photochemistry program funded by the Office of Science, Office of Basic Energy Sciences, Division of Chemical Sciences, Geosciences, and Biosciences.

## References and Notes

- (1) Kortan, A. R.; Hull, R.; Opila, R. L.; Bawendi, M. G.; Steigerwald, M. L.; Carroll, P. J.; Brus, L. E. *J. Am. Chem. Soc.* **1990**, *112*, 1327–1332.
- (2) Hines, M. A.; Guyot-Sionnest, P. *J. Phys. Chem.* **1996**, *100*, 468–471.
- (3) Dabbousi, B. O.; RodriguezViejo, J.; Mikulec, F. V.; Heine, J. R.; Mattoussi, H.; Ober, R.; Jensen, K. F.; Bawendi, M. G. *J. Phys. Chem. B* **1997**, *101*, 9463–9475.
- (4) Landes, C.; Burda, C.; Braun, M.; El-Sayed, M. A. *J. Phys. Chem. B* **2001**, *105*, 2981–2986.
- (5) Donega, C. D.; Hickey, S. G.; Wuister, S. F.; Vanmaekelbergh, D.; Meijerink, A. *J. Phys. Chem. B* **2003**, *107*, 489–496.
- (6) Micic, O. I.; Sprague, J.; Lu, Z. H.; Nozik, A. *J. Appl. Phys. Lett.* **1996**, *68*, 3150–3152.
- (7) van Sark, W.; Frederix, P.; Van den Heuvel, D. J.; Gerritsen, H. C.; Bol, A. A.; van Lingen, J. N. J.; Donega, C. D.; Meijerink, A. *J. Phys. Chem. B* **2001**, *105*, 8281–8284.
- (8) Soloviev, N. V.; Eichhofer, A.; Fenske, D.; Banin, U. *J. Am. Chem. Soc.* **2001**, *123*, 2354–2364.
- (9) Nirmal, M.; Dabbousi, B. O.; Bawendi, M. G.; Macklin, J. J.; Trautman, J. K.; Harris, T. D.; Brus, L. E. *Nature* **1996**, *383*, 802–804.
- (10) Banin, U.; Bruchez, M.; Alivisatos, A. P.; Ha, T.; Weiss, S.; Chemla, D. S. *J. Chem. Phys.* **1999**, *110*, 1195–1201.
- (11) Kuno, M.; Fromm, D. P.; Hamann, H. F.; Gallagher, A.; Nesbitt, D. J. *J. Chem. Phys.* **2000**, *112*, 3117–3120.
- (12) Ebenstein, Y.; Mokari, T.; Banin, U. *Appl. Phys. Lett.* **2002**, *80*, 4033–4035.
- (13) Maenosono, S.; Eiha, N.; Yamaguchi, Y. *J. Phys. Chem. B* **2003**, *107*, 2645–2650.
- (14) Maenosono, S.; Dushkin, C. D.; Saita, S.; Yamaguchi, Y. *Jpn. J. Appl. Phys., Part 1* **2000**, *39*, 4006–4012.
- (15) Maenosono, S.; Ozaki, E.; Yoshie, K.; Yamaguchi, Y. *Jpn. J. Appl. Phys., Part 2* **2001**, *40*, L638–L641.
- (16) Cordero, S. R.; Carson, P. J.; Estabrook, R. A.; Strouse, G. F.; Buratto, S. K. *J. Phys. Chem. B* **2000**, *104*, 12137–12142.
- (17) Hess, B. C.; Okhrimenko, I. G.; Davis, R. C.; Stevens, B. C.; Schulzke, Q. A.; Wright, K. C.; Bass, C. D.; Evans, C. D.; Summers, S. L. *Phys. Rev. Lett.* **2001**, *86*, 3132–3135.
- (18) Underwood, D. F.; Kippeny, T.; Rosenthal, S. J. *J. Phys. Chem. B* **2001**, *105*, 436–443.
- (19) Burda, C.; Link, S.; Mohamed, M.; El-Sayed, M. *J. Phys. Chem. B* **2001**, *105*, 12286–12292.
- (20) Lifshitz, E.; Glozman, A.; Litvin, I. D.; Porteanu, H. *J. Phys. Chem. B* **2000**, *104*, 10449–10461.
- (21) Peng, Z. A.; Peng, X. G. *J. Am. Chem. Soc.* **2001**, *123*, 183–184.

- (22) Murray, C. B.; Norris, D. J.; Bawendi, M. G. *J. Am. Chem. Soc.* **1993**, *115*, 8706–8715.
- (23) Phillips, D.; Drake, R. C.; Oconnor, D. V.; Christensen, R. L. *Anal. Instrum. (NY)* **1985**, *14*, 267–292.
- (24) Ellingson, R. J.; Blackburn, J. L.; Yu, P. R.; Rumbles, G.; Micic, O. I.; Nozik, A. J. *J. Phys. Chem. B* **2002**, *106*, 7758–7765.
- (25) Palmer, R. G.; Stein, D. L.; Abrahams, E.; Anderson, P. W. *Phys. Rev. Lett.* **1984**, *53*, 958–961.
- (26) Cohen, M. H.; Grest, G. S. *Phys. Rev. B* **1981**, *24*, 4091–4094.
- (27) Franceschetti, A.; Zunger, A. *Phys. Rev. B* **2000**, *62*, R16287–R16290.
- (28) Wang, L. W. *J. Phys. Chem. B* **2001**, *105*, 2360–2364.
- (29) Lindsey, C. P.; Patterson, G. D. *J. Chem. Phys.* **1980**, *73*, 3348–3357.
- (30) Norris, D. J.; Bawendi, M. G. *J. Chem. Phys.* **1995**, *103*, 5260–5268.
- (31) Efros, A. L.; Rosen, M.; Kuno, M.; Nirmal, M.; Norris, D. J.; Bawendi, M. *Phys. Rev. B* **1996**, *54*, 4843–4856.
- (32) Franceschetti, A.; Fu, H.; Wang, L. W.; Zunger, A. *Phys. Rev. B* **1999**, *60*, 1819–1829.
- (33) Nirmal, M.; Norris, D. J.; Kuno, M.; Bawendi, M. G.; Efros, A. L.; Rosen, M. *Phys. Rev. Lett.* **1995**, *75*, 3728–3731.
- (34) Bawendi, M. G.; Carroll, P. J.; Wilson, W. L.; Brus, L. E. *J. Chem. Phys.* **1992**, *96*, 946–954.
- (35) Rumbles, G.; Selmarten, D. C.; Ellingson, R. J.; Blackburn, J. L.; Yu, P. R.; Smith, B. B.; Micic, O. I.; Nozik, A. J. *J. Photochem. Photobiol., A* **2001**, *142*, 187–195.
- (36) Hoheisel, W.; Colvin, V. L.; Johnson, C. S.; Alivisatos, A. P. *J. Chem. Phys.* **1994**, *101*, 8455–8460.